Tunnel-convective air-assisted spraying technology for improving droplet deposition on hedgerow vines

Zhenjie Wen[1], Wei Qiu[1*], Zhentao Zhang[1], Weimin Ding[1], Xiaolan Lyu[2], Fiaz Ahmad[3], Hui Wang[1]

(1. *College of Engineering, Nanjing Agricultural University, Nanjing 210031, China*;
2. *Jiangsu Academy of Agricultural Sciences, Nanjing 210014, China*;
3. *Department of Agricultural Engineering, Bahauddin Zakariya University, Multan 60800, Pakistan*)

Abstract: Given the impermeability, larger dosage, and higher drift of pesticides used in modern hedgerow vine canopies, a novel tunnel-convective air-assisted spraying technology was proposed. Mechanized spraying equipment with high penetration and low drift was developed. The air-assisted system of this equipment was centrosymmetric, and the fan type was cross-flow. The fan outlet width was 138 mm and the air duct's main body followed a logarithmic spiral profile, based on parallel flow theory. The external diameter of the impeller was 157 mm, which was fixed into a barrel structure by 23 strong forward-curved blades, each being 1 mm thick. The central angle of the blades was 108°, and the ratio of the internal and external diameters was 0.81. The impeller and air duct served as guides to circulate and reciprocate airflow around the crown, forming a tunnel-convective air-assisted to the vine. Using MATLAB interpolation, the airflow trajectory of the air convection circulation in the door-shaped cover was obtained. The velocity field distribution test showed that, in the case of a canopy, there were tunnel-convective circulating airflows with high velocity on both sides and uniform velocity in the middle of the canopy. Due to the tunnel-convective air-assisted spraying technology, the vertical distribution uniformity of spray deposition has been significantly improved, spray penetration has been enhanced, penetrability has been effectively improved, and droplets on the ground and in the air have been significantly reduced. The results of this study can assist in providing further optimization and improvement of plant protection machinery. The new tunnel-convective air-assisted spraying technology may be a more favorable choice for future spray applications and the environment.

Keywords: plant protection, air-assisted, hedgerow vines, cross-flow fan, droplet deposition
DOI: 10.25165/j.ijabe.20211406.6482

Citation: Wen Z J, Qiu W, Zhang Z T, Ding W M, Lyu X L, Ahmad F, et al. Tunnel-convective air-assisted spraying technology for improving droplet deposition on hedgerow vines. Int J Agric & Biol Eng, 2021; 14(6): 9–18.

1 Introduction

For many years, chemical control of pests and pathogens has been a decisive factor in maintaining the high quality and yield of vineyards[1,2]. Hedgerow planting is the main form of vineyard cultivation. Its characteristics include having good light, ease of management, being suitable for close planting, and mechanized operation. Moreover, the branches grow according to the shape of the walls and their crown diameters are more consistent than the traditional canopy[3,4].

The majority of researchers have developed a tunnel-type spraying technology for the vineyard hedgerow planting mode[5, 6], which uses short-distance spraying across rows and intercepts the droplets that do not hit the target[7]. Owing to the short distance between the exit of the tunnel atomizer and the surface of the crop, the minimum distance between each other is 0.25-0.30 m[8]. In such a short distance, the conventional pressure spray is likely to cause the mist flow to concentrate, forming a striped and uneven spray. If the pressure is too small, the penetration of the droplets will be poor, and the deposition rate inside the canopy and abaxial leaf surfaces will be insufficient[9]. Therefore, air-assisted technology has been used to improve the distribution uniformity of droplets in the canopy[10,11]. An in-depth exploration of various single-sided, single-row, and double-row air-assisted tunnel sprayers has been done[12,13]. Axial fans have frequently been used for these purposes inside the tunnel. In one study, the tunnel sprayer used to spray dwarf apple trees was equipped with four axial fans installed on each side of the fruit tree, which significantly enhanced the energy of the droplets entering the canopy from all around[14]. Doruchowski and Holownicki proposed a mode of combining a single large axial flow fan with an external air duct, effectively reducing the number and weight of fans[15]. To solve the problem of offsetting the airflow energy inside the canopy when the airflow blew on both sides of the canopy at the same time, the arrangement of the air outlets on both sides was adjusted[16]. Moreover, Ade and Pezzi adopted an internal air duct structure[17], the axial fans on both sides of the tunnel discharged air in opposite directions, which optimized the air circulation performance in the air delivery system[18].

However, most of the air outlet methods studied in the past used multi-source point-spraying. In these methods, when spraying over a short distance, it is difficult to ensure that the droplets are evenly applied to all areas of the canopy; hence, there

Received date: 2021-01-25 **Accepted date:** 2021-09-06
Biographies: Zhenjie Wen, MS, research interests: pesticide application technology, Email: wenzhenjie@njau.edu.cn; **Zhentao Zhang,** MS, research interests: pesticide application technology, Email: 861673809@qq.com; **Weimin Ding**, PhD, Professor, research interests: agricultural machinery, Email: wmding@njau.edu.cn; **Xiaolan Lyu,** PhD, research interests: pesticide application technology, Email: lxlanny@126.com; **Fiaz Ahmad,** Postdoctoral Fellow, research interests: theory and design of agricultural machinery, Email: engrfiaz@yahoo.com; **Hui Wang,** BS, research interests: pesticide application technology, Email: 9173010417@njau.edu.cn.
***Corresponding author: Wei Qiu,** PhD, Associate Professor, research interests: pesticide application technology. College of Engineering, Nanjing Agricultural University, Nanjing 210031, China. Tel: +86-25-58606570, Email: qiuwei@njau.edu.cn.

is uneven distribution of droplets along the canopy height direction[19]. Considering the shortcomings of the spraying technology for hedgerow vines, a tunnel-convective air-assisted spraying technology is proposed for hedgerow vines in this study by utilizing the characteristics of uniform air output and slow airflow attenuation by cross-flow fans[20]. A pair of cross-flow fans was arranged in a centrosymmetric manner to guide the airflow in a multi-dimensional flow pattern and the disturbance in the canopy, which is assumed to improve the deposition uniformity and the spatial distribution of droplets in the canopy.

The objectives of the present research were to: (1) design a tunnel-convective air-assisted atomizer and the technical parameters of its key components; (2) explore the airflow distribution in the limited space formed by the air-assisted atomizer based on the out-of-phase arrangement of the cross-flow fan; (3) use canopy droplet deposition rate, drift loss, and liquid recovery as the evaluation index, compare the improvement effect of the model without air assistance and the tunnel-convective air-assisted spraying technology.

2 Materials and methods

2.1 Structure and working principle of the device

Modern vineyards generally adopt a flood irrigation hedgerow planting pattern with a canopy width of 0.6-0.8 m, row spacing of 2.3-2.5 m, vine height of 2.2-2.4 m, and plant spacing of 0.7-0.9 m[21,22]. In the present study, a Dongfeng tractor with 4.5×10^4 W (Changzhou Dongfeng Agricultural Machinery Group Co., Ltd., China) was used. It was connected to a traction platform, which carried a tunnel-convective air-assisted atomizer for spraying operations. The air-assisted atomizer mainly comprised an air-assisted system, a spray system, and an expansion door system. The structure of the device is shown in Figure 1. The air-assisted system included four cross-flow fans, two on each side of the rack. The airflow hoods of each pair of fans constituted a semi-enclosed door-shaped space for the passage of plants; the cross-flow fans were powered by hydraulic motors. The spraying system was driven by the tractor's power take-off (PTO) shaft; the nozzle was set on the vertical jet rod on the side of the air outlet of the cross-flow fan. In the expansion door system, through the hydraulic cylinder, the width of the single-sided cover (which the cross-flow fan was a part of) was modified to fall within the range of 0.9-1.7 m; the height was adjusted to fall within the range of 2.2-2.5 m.

When the machine was operated, the air-assisted system drove the airflow into the inflow arc of the initial cross-flow fan. Because of the impeller's movement, the airflow blew out from the outflow arc. The airflow penetrated the plants into the inflow arc of the cross-flow fan placed relative to them. After blowing out of the outflow arc, the air passed through the canopy again and entered the inflow arc of the initial cross-flow fan, which guided the airflow to circulate repeatedly in the canopy and form an air-assisted tunnel-convective effect. Then, the droplets sprayed by the nozzle were atomized again by the airflow and blown into the grape canopy. The atomizer was close to the surface of the crop; the droplets that were partially separated from the vine leaves were intercepted by the air-liquid separation device. After the air and liquid were separated, the droplets were collected before flowing into the liquid-receiving tank. When the liquid level in the tank reached the designated position, the liquid level switch sent a signal to the recovery liquid pump, and the residual liquid in the liquid-receiving tank was recovered to the recycling spray tank.

The main technical parameters of the atomizer are shown in Table 1.

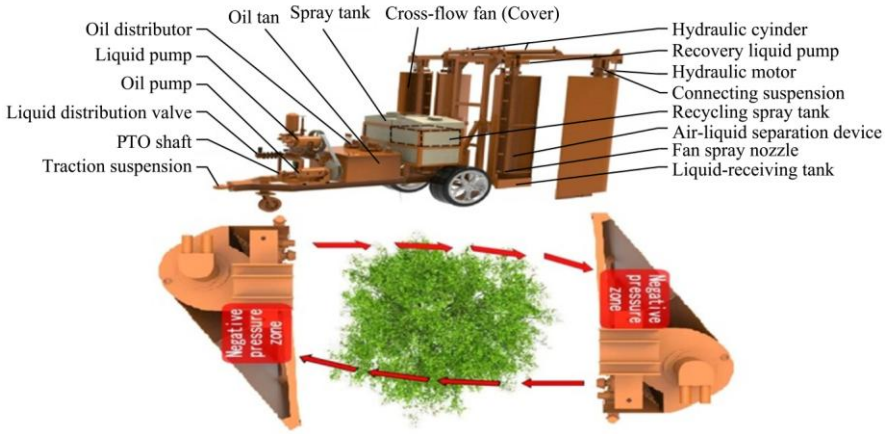

Figure 1 Structure of the tunnel-convective air-assisted atomizer

Table 1 Main technical parameters of the tunnel-convective air-assisted atomizer

Parameter	Value/Type
Dimensions (length × width × height)/mm×mm×mm	4600×4200×2700
Supporting power/W	4.5×10^4
Fan type	Cross-flow
Single cover height/mm	2200
Single cover width/mm	600
Boom height/mm	1700
Liquid pump type	Plunger pump
Spray tank volume/L	400
Recycling spray tank volume/L	50
Nozzle type	Fan spray
Working speed/m s^{-1}	0.8-2.0

2.2 Outlet width design based on turbulence theory

The outlet width of the cross-flow fan was a key factor for the outlet airflow velocity of the air-assisted sprayer. Meanwhile, airflow velocity affected the effect of pesticide adhesion on fruit tree targets. Scholars have studied an air-assisted atomizer with a single-sided cross-flow fan as the core component, and the test validated the plane jet model for the fan outlet airflow velocity[23]. However, unilateral spraying caused the canopy of grapevines to face bottleneck problems such as impenetrability, larger dosage, and higher drift of the liquid pesticide. If a fan of the same size is positioned on the opposite side of a single fan (i.e., staggered), the two fans would work together. Since the airflow velocity on the blowing side would be faster than that on the opposite suction side,

the airflow tended to flow into the suction side. At the same time, the airflow velocity on the suction side would be higher than that on the surroundings owing to the high-speed operation of the fan impeller on the suction side. According to the Bernoulli equation, the pressure on the suction side would be lower than ambient atmospheric pressure. For this reason, a negative pressure zone formed on the suction side in our experiment, which gradually increased the decayed airflow velocity on the blowing side[24, 25]. In this way, the airflow was blown out from one side and sucked in on the other side, and the airflow continuously circulated in the space for multi-dimensional flow, forming a new type of tunnel-convective air-assisted mode.

However, the plane jet model was no longer suitable for the analysis of the multi-dimensional flow air-assisted mode. Nevertheless, co-direction parallel flow theory, which is based on turbulence theory, guided the design of the outlet width of the tunnel-convective air-assisted atomizer[26-28]. The formula is as follows:

$$\frac{U_c - U_s}{U_o - U_s} = \frac{x_p}{x} \tag{1}$$

$$\frac{x_p}{B'} = 4 + 12\lambda \tag{2}$$

$$\lambda = \frac{U_s}{U_o} \tag{3}$$

where, U_c is the airflow velocity along the jet axis, m/s; U_o is the airflow velocity of the outlet, m/s; U_s is the velocity of the parallel flow, m/s; x is the distance from the outlet, m; B' is outlet width, m; x_p is length of the potential core, m; λ is flow rate ratio.

Based on unilateral cross-flow fan research, the outlet velocity of the airflow should reach 11 m/s to atomize the droplets fully[23]. However, because of the requirements of the air-assisted orchard sprayer's droplet deposition density, airflow velocity of 8-9 m/s reaching the outside of the vine (U_c) was more suitable[29]. When using Equation (1), U_c was taken as 9 m/s. The distance from the air outlet to the outside of the canopy represents the sum of the canopy thickness (0.8 m) and spray distance (0.3 m), with the total value being 1.1 m. U_s was equal to 2 m/s, which represented the parallel airflow velocity near the canopy surface on the suction side. Together, Equations (1)-(3) can be used to obtain the outlet width of the tunnel-convective air-assisted atomizer. The outlet width (B') was taken as 0.138 m.

2.3 Air duct design theory

The cross-flow fan mainly consisted of an impeller, an air duct, and a vortex wall, as shown in Figure 2. The airflow field formed by the normal operation of the fan mainly included two areas: the eccentric vortex and cross-flow. An eccentric vortex appeared near the vortex wall away from the center of the impeller. Under the guidance of the air duct, the airflow around the eccentric vortex formed a transverse flow and discharged along the extension line of the rear wall. The cross-flow blew and flipped the canopy blades; it carried the droplets from the nozzle so that they would evenly penetrate the vine.

To guide the airflow to the cross-flow area and obtain a uniform velocity distribution, it was necessary to consider the size of the air duct in detail and determine the parameters of each component in the duct. The air duct consisted of three parts, as shown in Figure 2. The first part was the inflow arc tangential to the rear wall. The rear wall responsible for wrapping the impeller was the second part, and the third part was the section carrying the outflow section of the rear wall. The first and third parts were both tangent to the second part. The curve of the rear wall of the second part had to be carefully considered. Research shows that the air resistance of the airflow can effectively be reduced using a logarithmic spiral profile[30] and that doing this is more conducive to an ideal fluid reaching the laminar flow state. With the help of laminar flow, the droplets can be uniformly dispersed, improving the deposition and adhesion performance. The logarithmic spiral formula is defined as follows:

$$R = R_a e^{\theta/\theta^*} = R_2(1 + \frac{e_R}{R_2})e^{\theta/\theta^*} \tag{4}$$

where, R_a is the radial distance from the center of the impeller to the starting point of the rear wall, mm; R_2 is the outer radius of the impeller, mm; e_R is the radial clearance between the rear wall and the impeller, mm; θ^* is the rear wall radial width, (°); θ is the angle rotated counterclockwise from the starting point of rear wall, (°).

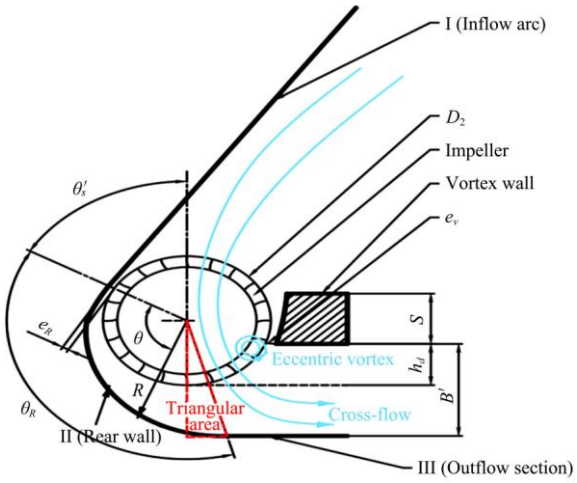

Figure 2 Airflow trajectory and duct parameters of the cross-flow fan

In the design of a cross-flow fan[31], the rear wall radial width is the basic parameter that affects the characteristic curve of the fan. It can have three values depending on the size of the rear wall radial width: θ^*=139°, θ^*=191°, and θ^*=359°. The fan performance curve with a relatively large flow coefficient can be obtained using the rear wall of the intermediate numerical radial width. For this reason, θ^*=191°was chosen.

To perform a more in-depth analysis, a few more parameters need to be introduced: θ_s' is the angle from the vertical axis of the impeller to the starting point of the rear wall, °; θ_R is the logarithmic spiral profile covering angle, °; S is the vortex wall thickness, mm; e_V is the radial gap between the vortex wall and the impeller, mm; D_2 is the outer diameter of the impeller and h_d is the height of the vortex wall, mm. When e_R/D_2 is equal to 0.04, θ_s' is equal to 60°, θ_R is equal to 135°, and the fan performance is relatively stable[31]. To determine the thickness and position of the plane vortex wall, related studies have shown that the radial clearance between the vortex wall and the impeller has little effect on the performance of the fan. Following one study, e_V/D_2 was taken as 0.07[32]. The gap shape was modeled as an arc and a thicker vortex wall was selected, which tends to minimize the resistance of the eccentric vortex to the upward airflow and improve the efficiency of the fan. To improve the total pressure effectively, S/D_2 was taken as 0.39. The flow field in the duct was not axisymmetric. The highest radial velocity was located near the edge of the vortex wall. Large flow fluctuation existed in the area near the vortex wall which led to prominent fan noise problems. The noise of the cross-flow fan can be reduced by

setting the height of the vortex wall h_d/D_2 to 0.32 m[33].

The aforementioned fan outlet width was 138 mm, and there was a triangular area inside the impeller and rear wall. The outer radius of the rotor can be obtained from the trigonometric function:

$$R_2 = R_{\theta_R} \times \cos(135° - 90° - 30°) + h_d - B' \quad (5)$$

R_2 was calculated as 78.6 mm using Equations (4)-(5), which means D_2 was 157 mm. The following data can be calculated: e_R=0.04D_2=6 mm, e_V=0.07D_2=11 mm, S=0.39D_2=61 mm, and h_d=0.32D_2=50 mm.

2.4 Impeller design theory

In this study, the working airflow generated by the rotation of the fan impeller had to drive out and completely replace all of the air contained in the door-shaped tunnel. The blades of the impeller had a circular arc profile, which conformed to the strong forward curvature necessary for the air to flow through the blade twice, in accordance with aerodynamic theory. Considering the compactness of the overall structure of the fan, it was necessary to determine the inner diameter of the impeller (D_1), central angle of the blade (δ), inner and outer angles of the blade (β_1, β_2), inside installation radius of the blade (R_ρ), positioning radius of the blade center (R_0), pitch of the blade (t), and number of blades (Z). These variables are shown in Figure 3.

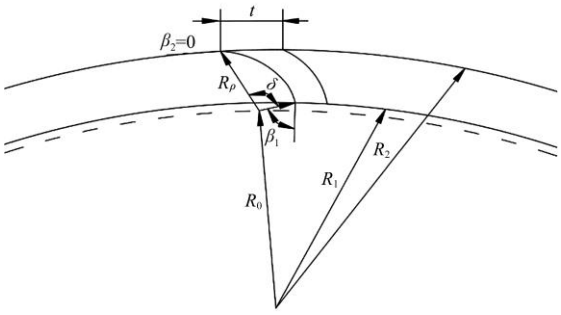

Figure 3 Impeller geometry parameters

The outer diameter of the impeller largely determines the overall dimensions of a single cross-flow fan. From the aforementioned calculation results, it is determined that D_2 is equal to 157 mm. To obtain a larger flow coefficient, a larger value $\overline{D_1}$ of the relative diameter of the blade inlet should be selected ($\overline{D_1} = D_1 / D_2 = 0.7 - 0.85$), $\overline{D_1}$ is equal to 0.81 and D_1 is equal to 127 mm. The size of the blade center angle (δ) directly affects the flow channel form of the air-assisted device; its relationship with the inner and outer angles of the blade is as follows:

$$\delta = 180° - (\beta_1 + \beta_2) \quad (6)$$

The change in the impeller blade angle does not have a significant impact on the total pressure of the fan, but it evidently has an influence on the maximum efficiency and flow rate of the fan. The internal blade angle (β_1) should not be too small because flow separation loss occurs when the airflow enters the blade. If the duct is designed as an accelerated channel, the blade center angle (δ) is greater than 90°. δ was chosen as 108° and β_1 was chosen as 72°, following previous research and experiments[34]. From Equation (6), the outer blade angle (β_2) was set to 0°. The installation radius inside the blade (R_ρ) and the positioning radius of the blade center (R_0) can be used to calculate the forward blade of the fan using the following formulas:

$$R_\rho = \frac{R_2^2 - R_1^2}{2(R_2 \cos\beta_2 - R_1 \cos\beta_1)} \quad (7)$$

$$R_0 = \sqrt{R_\rho^2 + R_1^2 - 2R_\rho R_1 \cos\beta_1} \quad (8)$$

where, R_2 is the outer radius of the impeller and R_1 is the inner radius of the impeller, mm. Once R_2 and R_1 are substituted into Equation (7) and Equation (8), it is found that R_ρ is 18 mm and R_0 is 60 mm.

In a cross-flow fan impeller, the blade pitch (t) is equal to R_ρ; thus, t is 18 mm. The number of blades affects the flow diversion between the blades. According to the formula, Z=πD_1/t=22.2, the number of blades is 23, and the thickness of the blade is 1 mm. A single blade was fixed by the blade ring, and the impeller shaft sleeve locked the blade ring, forming a complete cross-flow fan impeller.

2.5 Design of the liquid recovery system

The liquid recovery system includes air-liquid separation devices, liquid-receiving tanks, liquid level switches, strainers, collecting pipes, recovery liquid pumps, and a recycling spray tank. The air-liquid separation device was fixed at the inlet and outlet of the cross-flow fan to protect the cross-flow fan and collect the droplets that were not deposited on the target. The liquid-receiving tank was located at the bottom of the cross-flow fan and used to retrieve the lost liquid from the target. The liquid level switch was placed in the setting position of the liquid-receiving tank. The recycling spray tank was placed on the traction platform on the front side of the doorframe.

During operation, the tractor's power supply provided power to the recovery liquid pump. The droplets separated from the target were collected in the liquid-receiving tank through the air-liquid separation device, and the collection pipe passed into the liquid-receiving tank. The end of the collection pipe was equipped with a strainer to prevent it from being blocked by branches, blades, and dirt. The workflow is illustrated in Figure 4. A liquid level switch was fixed in the middle of the bottom of the liquid-receiving tank. When the liquid reached the set height, the microswitch closed, and the recovery liquid pump started to operate. After the impurities had been filtered out, the liquid was recovered to the recycling spray tank through the collection pipe. When the liquid level dropped to the depth below 5 cm, the microswitch disconnected, and the recovery liquid pump stopped working to prevent idling, which could damage the recovery liquid pump.

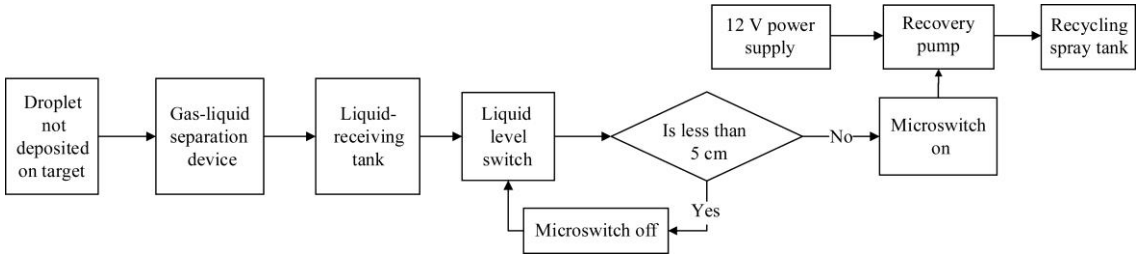

Figure 4 Liquid recovery system

2.6 Test design

The goal of the test was to study the airflow trend in the door-shaped cover and the velocity distribution of the airflow in the canopy under the air-assisted condition of the tunnel-convective

air-assisted atomizer. During the entire test phase, the equipment was in a relatively static state, and the airflow direction and airflow velocity were used as indicators to analyze the tunnel-convective air-assisted method of the device with and without a canopy. Based on the determination of the convective airflow field in the canopy, the deposition behavior of the droplets on the canopy, the change in the amount of spray drifting, and the amount of liquid recovery have been explored. These results have been done under the mode with and without air assistance.

2.6.1 Airflow direction distribution test

When the airflow was ejected from the cross-flow fan, the airflow carried droplets into the target. The direction of the airflow was closely related to the drift, deposition, and recovery of droplets. In this test, the fan was 1000 r/min, and the distance between the door-shaped cover was 1.4 m. The airflow direction was used as an evaluation index to analyze the movement trend of the airflow field.

As the cover was 0.3 m above the ground and the height of the liquid-receiving tank was 0.2 m, a level ruler and a handheld ultrasonic airflow direction instrument (JL-03-S1, Qing Yi Electronic Technology Co., China) were used at heights of 0.5 m, 1.0 m, 1.5 m, and 2.0 m above the ground. A horizontal sampling layer was set within each vertical height range (*Z*-axis). On each horizontal sampling layer, sampling points were set at intervals of 0.35 m along the horizontal direction of the outlet (*Y*-axis), and five points were taken. As the total width of the cross-flow fan was 0.6 m on one side, four points could be collected at intervals of 0.16 m when the fan width (*X*-axis) was 0.06 m away from the outlet. In this way, there were 20 points on each horizontal layer, and the sampling points of each layer were numbered 1-20, with a total of 80 sampling points. This is shown in Figure 5.

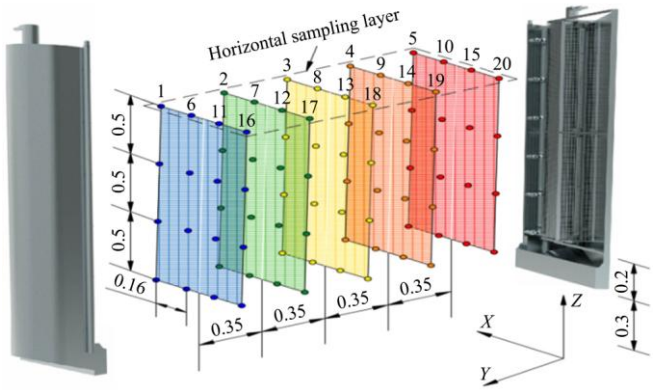

Figure 5 Dot layout inside the door-shaped cover (m)

When the measurements were taken, the ultrasonic airflow direction instrument was placed horizontally on each sampling point such that the north key of the instrument was facing the north, the direction of true north was 0 °, and the data increased clockwise (90 ° in the direction of true east). To take a reading, the start button had to be pressed and the person holding the instrument had to stay at the collection point for five seconds. Then, the angle value was displayed on the LCD screen of the measuring instrument. Each data point was measured three times, and the average value was taken as the direction of airflow in the area where the point was located. The airflow direction data of each test point are recorded hierarchically, and the angle of each sampling point was represented by an arrow line in Matlab. The midpoint of the arrow line was fitted with a polyfit function to obtain an interpolated function curve. These function curves can reflect the general trend of the airflow field in each layer. From this, the distribution of the flow field in the limited space of the air-assisted device can be demonstrated.

2.6.2 Airflow velocity distribution test in the canopy

Because of the limited space of the tunnel that needed to accommodate crops during operation, it was necessary to determine whether the existence of the canopy would destroy the formation of the airflow field. Therefore, the airflow field distribution in the canopy was evaluated based on the airflow velocity.

The experiment was carried out in standardized hedgerow-type vineyards of the West Industrial Development Center of Xinjiang Uyghur Autonomous Region. During this period, the vines were close to maturity; the leaves were dense and the canopy was large. The width of the vines in the garden was 0.8 m, the row spacing was 2.4 m, the canopy height was 2.4 m, the plant spacing was 0.8 m, and the average leaf area index was 2.8 m. The fan speed of the test equipment was set at 1000 r/min. Considering the size of the vineyard canopy, the distance between the door-shaped cover was set to 1.4 m, and the air outlet was 0.3 m away from the surface of the vine. The layout plan shown in Figure 5 was used. A TSI-9545 hot-wire anemometer (TSI Inc., Minnesota, USA) was used to measure the airflow velocity at each point. Each data point at each of the four different heights was measured three times, and the average value was taken as the airflow velocity value of the point. The data were sorted to describe the airflow velocity change curve of the airflow field.

2.6.3 Droplet deposition and drift test

The existence of a convective airflow field in the canopy was measured to verify further the influence of the tunnel-convective air-assisted atomizer on the droplet deposition rate under the air-assisted state. Referring to the method specified in ISO 22522 (ISO,2007), the application effects of the machine with and without the airflow field were compared. The experiment was also carried out in the hedgerow-standardized vineyard of the West Industrial Development Center of Xinjiang Uyghur Autonomous Region.

The left and right sides of the door-shaped cover were arranged symmetrically, and the working modes on both sides were completely consistent. The working condition of the right door-shaped cover of the air-assisted atomizer was regarded as the research object along the direction of machine travel. According to the characteristics of the uniform growth of the trees on the vertical hedgerow, the vines were intertwined with each other. Three vines with continuous growth were selected to set layout points. Along the height direction of the canopy, the upper, middle, and lower planes were selected as layer 1 (2.2 m), layer 2 (1.4 m), and layer 3 (0.6 m), respectively. Three surfaces were arranged with an interval of 0.8 m on the plumb surface in the working direction of the machine. Within the canopy, three sides from the left, middle, and right were selected at 0.3 m intervals along the spraying direction of the device. The intersection point of the horizontal and vertical planes served as the layout point. These points are represented by red points in Figure 6. Nine points were placed on each tree, with a total of 27 points. A test paper card (76×76 mm, M&G Stationery Inc., Shanghai, China) was placed on the leaf surfaces at the sample points.

The ground loss and air drift of droplets or particles are important factors affecting pesticide application; excess pesticide in the air and ground will cause pesticide waste and environmental pollution. Drift and droplet deposition tests were carried out simultaneously. Referring to the method specified in ISO 22866 (ISO, 2005), sampling points were arranged directly below the crop line and downwind along the spray route. A sampling point was

placed at the root of each plant along the line of work. These are shown in yellow in Figure 6. Spray drift was measured in the downwind area from the outside of the vine canopy. A total of four sampling points were set at intervals of 0.5 m. Sampling points were set at 0.8 m intervals along the working direction of the machine, and a total of three points were arranged. The drift rod was placed at a distance of 2 m away from the canopy. The sampling points on the rod were 0.6 m apart. A total of nine points were taken from the three rods. The test paper card (76 mm×76 mm, M&G Stationery Inc., Shanghai, China) was fixed at the sample point. A total of 24 sample points were used for the drift tests.

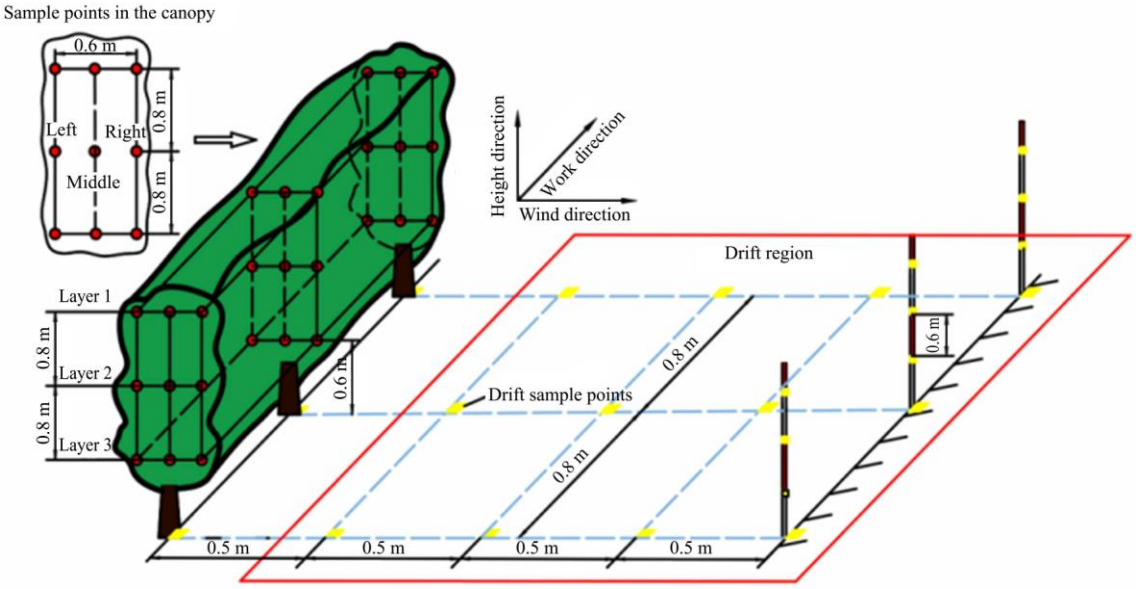

Figure 6 Deposition and drift test points

The test took place on September 18-29, 2019. The outside weather was adequate, and the average airflow velocity was less than 2 m/s. The test site is shown in Figure 7.

a. Front of atomizer b. Back of atomizer

Figure 7 Field test site

At the beginning of the test, the marked test paper was fixed to each sampling point using paper clips. The experimental parameters of the test were shown in Table 2. The spraying liquid was a Ponceau 2R aqueous solution with a mass fraction of 5‰ (SSS Reagent Co., Ltd., Shanghai, China). It was performed once with and without the air assistance mode, and each group of tests was repeated three times.

Table 2 Experimental parameters for the test

Factor	Value
Working speed/m s^{-1}	1
Spray pressure/MPa	0.5
Fan speed/r min^{-1}	1000
Door-shaped cover distance/m	1.4

After the operation, the paper cards were classified and packed into plastic zip sealing bags before being brought back to the laboratory. The Ponceau on the test paper cards at each sample point was dissolved in deionized water. The droplet deposition rate per unit area of all sample points inside and outside the canopy was calculated using an ultraviolet-visible spectrophotometer (UV2000, Unico Instrument Co., Ltd., Shanghai, China).

2.6.4 Liquid recovery test

In order to show the change in the liquid recovery under the air-assisted state, the tunnel-convective air-assisted atomizer was tested for the residual liquid recovery rate. The field test time was two minutes, and the total amount of liquid Q_s in the test process was recorded by an electronic flowmeter in the liquid path system. The value obtained was 22 320 mL. The level switch was closed in the liquid-receiving tank before the test. All residual liquid in each tank was collected and sent to the recycling spray tank by the recovery pump. Δ_r is defined as the change in volume of the liquid in the recycling spray tank. The liquid medicine recovery rate can be calculated as follows: $R=(\Delta_r/Q_s)\times100\%$. In each mode, each test group was repeated three times to obtain the mean value.

3 Results and discussion

3.1 Analysis of airflow field test results

Four horizontal sample layers with different heights in the vertical plane were fitted using MATLAB interpolation. The results of the airflow direction movement in the airflow field are presented in Figure 8a. From the airflow movement track, it can be seen that each side of the airflow was ejected from the outlet of the cross-flow fan at an angle close to 90°. Theoretically, the horizontal outflow airflow should be blown vertically. Because there was only a vortex wall between the fan outlet and the air inlet, the negative pressure of the inlet on the same side slightly influenced the direction of the outlet airflow. At the farthest distance from the air outlet of the fan, that is, at the end of the air inlet of the fan on the opposite side (sampling points 1 and 20 in Figure 5), the airflow was less affected by the negative pressure zone of the air inlet. However, it was affected by the atmospheric pressure outside the door-shaped cover; the airflow direction angle tended to flow out of the door cover, but it had little effect on the entire device. Therefore, these positions were not considered in the calculation when the motion trajectory was fitted. From sample points 6-11 and 15-10 on each side, it can be seen that the

direction of the airflow changed suddenly when the airflow was about to enter the center of the impeller, close to the vortex wall, the maximum deflection angle changed by 39°. This indicates that an eccentric vortex was formed near the vortex wall of the cross-flow fan, and that the negative pressure area generated by the high-speed flow of air near the eccentric vortex could press air into the impeller to achieve air circulation. As shown in Figure 8b, the airflow field trajectory at each level shows the trend of air convection. This cyclic reciprocating motion guided the multi-dimensional airflow in the door-shaped cover space, which contributed to the tunnel-convective air-assisted effect.

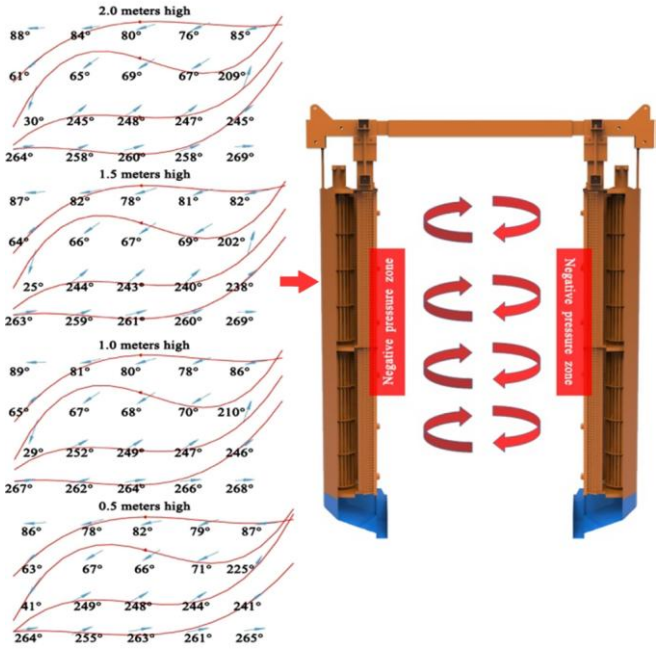

a. Airflow track profile b. Air movement in the tunnel

Figure 8 Movement trajectory of four height airflow fields in the door-shaped cover

The airflow velocity distribution data at each test point in the canopy is shown in Figure 9. The average airflow velocity at both sides of the air-assisted device was 11.33 m/s and 11.16 m/s. The airflow velocity from the outlet of the fan to the surface of the vine (corresponding to the position of sampling points 4 and 17 in Figure 5) attenuated itself. The average airflow velocity was 8.13 m/s and 8.03 m/s, which met the requirements of the final speed of the air entering the vine[35]. Because points 10 and 11 were close to the vortex wall, the airflow velocity was relatively high owing to the negative pressure area generated by the eccentric vortex. The speeds of sampling points 1 and 20 were less than 2 m/s. The area where these two test points were located was at the farthest air inlet position from the air outlet of the fan, which was less affected by the fan. Compared with the middle layer, the leaves at the top and bottom ends of the vine were sparser and were less of a hindrance to airflow. Therefore, the average airflow velocity on the test surfaces at both ends (Figures 9a and 9d) was greater than that on the middle layer (Figures 9b and 9c). By combining the velocity field distributions of different heights, a convective circulation of high airflow velocity on both sides and a uniform airflow in the middle of the canopy when the air-assisted device was working were found. As the pair of fans of the device started to work, the airflow blew from the outlet side to the suction port of the other fan. The airflow should have been rapidly attenuated by various factors in space and field, but the data showed that the outlet airflow velocity first decreased and then increased. It is more accurate to indicate that there were negative pressure zones on each side of the cross-flow fan in the staggered arrangement to guide the whirling movement of the airflow. Therefore, the presence of a convective airflow field in the canopy lays the foundation for field test research comparing devices with and without air assistance.

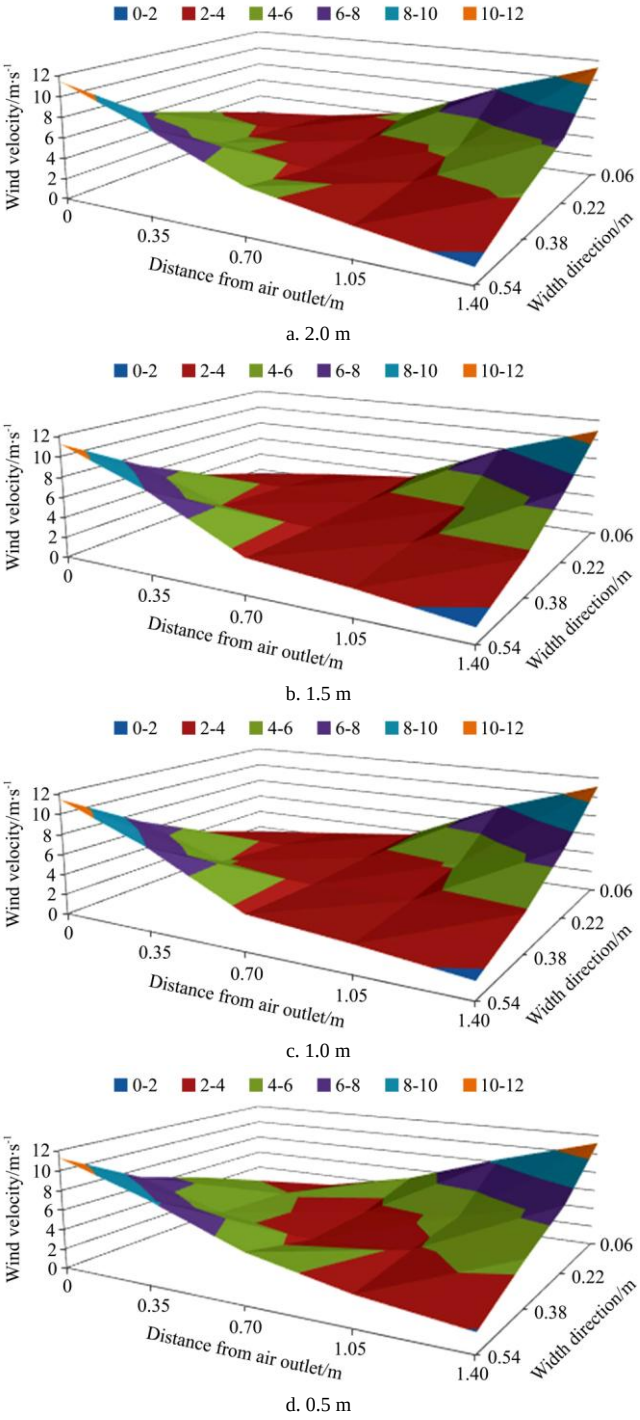

a. 2.0 m

b. 1.5 m

c. 1.0 m

d. 0.5 m

Figure 9 Airflow velocity distribution at four heights in the canopy at different height

3.2 Analysis of the test results of droplet deposition and drift

The average values of the three tests on the adaxial and abaxial surfaces of all sample points on the three vines were selected and recorded as the data of the droplet deposition. In Tables 3 and 4, the droplet deposition data on the adaxial and abaxial leaf surfaces in the canopy with/without air assistance are presented.

According to the analysis of the data of sample layers with different heights (Tables 3 and 4), the droplet deposition rate in

vine layer 3 was more than that in layers 1 and 2, especially when there was no air assistance. In the absence of air assistance, the initial velocity of the droplets after atomization from the nozzle was relatively slow. The droplets moved to the middle and lower parts of the canopy under the influence of gravity, which increased the accumulation of droplet deposition rate at the bottom of the canopy. From the data on the middle side of the vine, the droplet deposition rate on the lower part of the adaxial leaf was 2.43 times higher than the upper part, whereas on the abaxial leaf, the lower part was 1.72 times higher than the upper part. Compared with the mode without air assistance, the cross-flow fan set relative to the plants could generate a cyclic convection airflow. The air outlet mode was uniform, which improved the deposition uniformity of the droplet at different heights of the canopy. The CV of the vertical sample layer on the adaxial leaf in the middle of the canopy was reduced by 10.30%, and the CV of the vertical sample layer on the abaxial leaf was reduced by 4.02%.

Table 3 Droplet deposition rate on the adaxial leaf surfaces in the canopy

Sample group	With air assistance			Without air assistance		
	Left	Middle	Right	Left	Middle	Right
Layer 1 (μg/cm^2)	13.72	6.47	13.24	10.63	3.86	9.80
Layer 2 (μg/cm^2)	18.99	7.17	16.65	13.61	4.37	11.34
Layer 3 (μg/cm^2)	19.24	12.81	17.32	17.53	9.39	14.09
Mean (μg/cm^2)	17.32	8.82	15.74	13.92	5.87	11.74
CV (%)[a]	14.70	32.19	11.35	20.29	42.29	15.11

Note: [a] CV=coefficient of variation of sample points at three vertical heights.

Table 4 Droplet deposition rate on the abaxial leaf surfaces in the canopy

Sample group	With air assistance			Without air assistance		
	Left	Middle	Right	Left	Middle	Right
Layer 1/μg cm^{-2}	9.46	4.75	8.71	7.93	2.97	6.41
Layer 2/μg cm^{-2}	10.81	5.24	8.97	9.40	3.68	7.81
Layer 3/μg cm^{-2}	10.90	7.23	9.65	10.21	5.11	9.52
Mean/μg cm^{-2}	10.39	5.74	9.11	9.18	3.92	7.91
CV/%[a]	6.34	18.68	4.35	10.28	22.70	16.07

Note: [a] CV=coefficient of variation of sample points at three vertical heights.

By averaging the droplet deposition rate from the vertical sample layers (Figure 10), the droplet deposition rate on both sides of the leaves inside and outside the canopy showed a high distribution on each side and a low distribution in the middle. And the average value of droplet deposition rate on the left side was higher than that on the right side. The device was used for riding in the field, and the direct working area of the vertical spray boom set on the left cross-flow fan was regarded as the left side of the crop. The left boom was closer to the main body of the machine, and the working distance of the liquid pump was short. The right boom was at the far end of the entire device. The pipeline from the liquid pump to the right boom was longer. The bending of the pipe led to an increase in the liquid loss along the way, which caused the hydraulic flow deviation inside the canopy to result in different droplet deposition rate on each side of the canopy. By comparing the average value of the middle part of the canopy vertical sample layer with and without air assistance, it can be seen that under the multi-dimensional flow and disturbance of convective airflow in the tunnel, the jet penetration was enhanced and the penetration was improved. The deposition rate of droplets on the adaxial leaf in the middle of the canopy increased by 50.26%, and the deposition rate of droplets on the abaxial leaf increased by 46.43%.

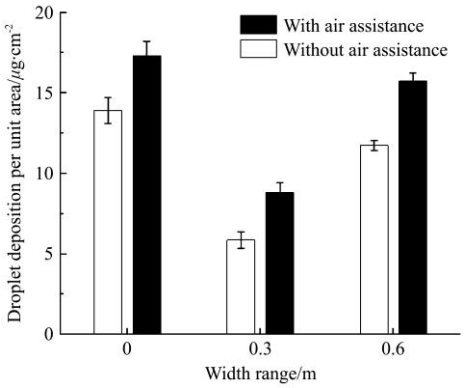

a. On the adaxial leaf

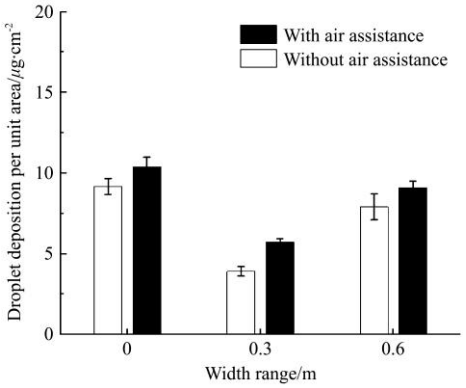

b. On the abaxial leaf

Figure 10 Droplet deposition rate along the width

The average value of the ground deposition rate data of the vines obtained in the drift test is plotted as a broken line in Figure 11. The analysis shows that the droplet loss of the entire device is mainly concentrated between the operating rows. In the state without air assistance, the liquid loss on the ground of the machine is 1.46 times that of the air outlet mode. This indicates that when the droplets were sprayed from the nozzle, owing to the characteristics of the prevention and control target, a kind of "wall" was formed on the outside of the canopy, which hindered the sprayed droplets. For this reason, low-speed droplets could not enter the tree body, causing a large number of droplets to deposit on the roots of the canopy forming ground loss between the working rows. When the tunnel-convective air-assisted mode was used for spraying, the droplet loss on the ground was greatly improved, and the total ground droplet loss was reduced by 37.51%.

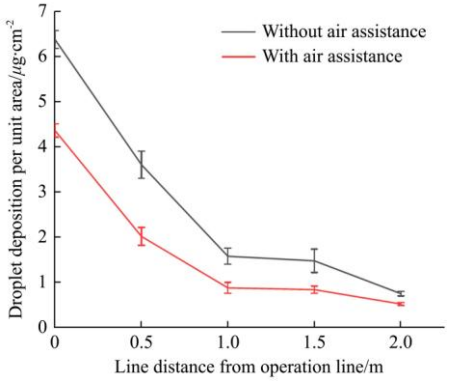

Figure 11 Liquid ground drift

The drift data of the air droplets are listed in Table 5. The average drift of the droplets is 0.52 μg/cm^2 and 0.74 μg/cm^2 with and without air assistance, respectively. In the case of air assistance, the droplet drift in the air was reduced by 29.73%.

Table 5 Air drift data of droplets

Working condition	Air drift/μg cm^{-2}		
	0.6 m above the ground	1.2 m above the ground	1.8 m above the ground
Without air assistance	0.88	0.68	0.67
With air assistance	0.65	0.65	0.27

3.3 Analysis of liquid recovery results

In the residual liquid recovery test, the recovery rate results of the device are shown in Table 6.

Table 6 Liquid recovery rate under different working conditions

Working condition	Change of liquid inside the recycling spray tank/mL	Liquid recovery rate/%
Without air assistance	2710	12.14
With air assistance	3120	13.98

From Table 6, we can see that because of the convective airflow in the tunnel, the recovery rate of the liquid of the equipment increased by 1.84% compared with the mode without air assistance. As the grape-harvesting season approached, the canopy leaves were dense, and the individual leaves were relatively large. Therefore, the recovery rate of the residual liquid was not high when the liquid was mostly retained in the canopy. The difference in recovery rates under the two working conditions was not significant. When the air-assisted mode was not activated, part of the liquid could be directly recovered by the liquid-receiving tank on the side because it did not enter the plant canopy. In the air-assisted state, the droplets entered the canopy with the airflow, and excess droplet deposition was collected on the other side. In the test, some liquid droplets adhered to the inner wall of the cover and did not fall into the liquid-receiving tank. This series of circumstances resulted in a relatively similar collection for both modes.

4 Conclusions

In this study, a novel type of tunnel-convective air-assisted spraying technology was proposed. A pair of cross-flow fans was arranged in a centrosymmetric manner, and the impeller and air duct guided the airflow to circulate and reciprocate itself around the crown, forming a tunnel-convective air-assisted effect on the vines. The droplets entered inside the canopy of the vine along with the turbulent airflow, breaking through the droplet deposition in the inner canopy and the back of the leaves.

To fulfill the plant protection and ecological requirements of hedgerow vines, a novel and suitable type of cross-flow fan with a uniform transverse air outlet was designed and developed. The logarithmic spiral profile of the fan caused the airflow to flow laminarly.

Field test results show that, compared with the model without air assistance, the uniformity of the spray deposition vertical distribution significantly improved and the penetration was enhanced under the influence of tunnel convection. In the middle side of the canopy, the droplet deposition rate on the adaxial leaf surfaces increased by 50.26%, and that on the abaxial leaf surfaces increased by 46.43%. The droplet drift on the ground was reduced by 37.51%, and the drift in the air was reduced by 29.73%. A total of 13.98% of the sprayed liquid could be recovered under normal operating conditions.

Air-assisted spraying technology was applied for high penetration in the canopy and maximum deposition on the target. The proposed novel tunnel-convective spraying technology will be a favorable choice for future spray applications and sustainable environments.

Acknowledgements

This work was co-financed by the National Natural Science Foundation of China (Grant No. 51805271), Jiangsu Agricultural Science and Technology Innovation Fund (CX203172, CX181007), 'Qinglan Project' of Jiangsu Province (QLGC) and the Fundamental Research Funds for the Central Universities (KYXK2021001).

[References]

[1] Viret O, Siegfried W, Holliger E, Raisigl U. Comparison of spray deposits and efficacy against powdery mildew of aerial and ground-based spraying equipment in viticulture. Crop Prot, 2003; 22(8): 1023–1032.

[2] Diaconu A, Tenu I, Rosca R, Carlescu P. Researches regarding the reduction of pesticide soil pollution in vineyards. Process Saf Environ Prot, 2017; 108: 135–143.

[3] Ade G, Molari G, Rondelli V. Recycling tunnel sprayer for pesticide dose adjustment to the crop environment. Transactions of the ASABE, 2007; 50(2): 409–413.

[4] Pascuzzi S, Cerruto E, Manetto G. Foliar spray deposition in a "tendone" vineyard as affected by airflow rate, volume rate and vegetative development. Crop Prot, 2017; 91: 34–48.

[5] Hogmire H W, Peterson D L. Pest control on dwarf apples with a tunnel sprayer. Crop Prot, 1997; 16(4): 365–369.

[6] Fox R D, Derksen R C, Zhu H, Brazee R D, Svensson S A. A history of air-blast sprayer development and future prospects. Transactions of the ASABE, 2008; 51(2): 405–410.

[7] Svensson S A, Brazee R D, Fox R D, Williams K A. Air jet velocities in and beyond apple trees from a two-fan cross-flow sprayer. Transactions of the ASAE, 2003; 46(3): 611–621.

[8] Song J, He X, Zhang J, Liu Y, Zeng A. Design of Π-type recycling tunnel sprayer. Transactions of the CSAE, 2012; 43(4): 31–36. (in Chinese)

[9] Badules J, Vidal M, Bone A, Llop J, Salcedo R, Gil E, et al. Comparative study of CFD models of the air flow produced by an air-assisted sprayer adapted to the crop geometry. Comput Electron Agric, 2018; 149: 166–174.

[10] Panneton B, Lacasse B, Piche M. Effect of air-jet configuration on spray coverage in vineyards. Biosyst Eng., 2005; 90(2): 173–184.

[11] Molari G, Benini L, Ade G. Design of a recycling tunnel sprayer using CFD simulations. Transactions of the ASAE, 2005; 48(2): 463–468.

[12] Jamar L, Mostade O, Huyghebaert B, Pigeon O, Lateur M. Comparative performance of recycling tunnel and conventional sprayers using standard and drift-mitigating nozzles in dwarf apple orchards. Crop Prot, 2010; 29(6): 561–566.

[13] Planas S, Solanelles F, Fillat A. Assessment of recycling tunnel sprayers in Mediterranean vineyards and apple orchards. Biosyst Eng. 2002; 82(1): 45–52.

[14] Peterson D L, Hogmire H W. Tunnel sprayer for dwarf fruit trees. Transactions of the ASAE, 1994; 37(3): 709–715.

[15] Doruchowski G, Holownicki R. Environmentally friendly spray techniques for tree crops. Crop Prot, 2000; 19(8-10): 617–622.

[16] Holownicki R, Doruchowski G, Swiechowski W. Uniformity of spray deposit within apple tree canopy as affected by direction of the air-jet in tunnel sprayers. J Fruit Ornamental Plant Res Skierniewice (Poland), 1997; 5(3-4): 129–136.

[17] Ade G, Pezzi F. Results of field tests on a recycling air-assisted tunnel sprayer in a peach orchard. J Agric Eng Res, 2001; 80(2): 147–152.

[18] Ade G, Molari G, Rondelli V. Vineyard evaluation of a recycling tunnel sprayer. Transactions of the ASAE, 2005; 48(6): 2105–2112.

[19] Pergher G, Gubiani R, Cividino SRS, Dell'Antonia D, Lagazio C. Assessment of spray deposition and recycling rate in the vineyard from a new type of air-assisted tunnel sprayer. Crop Prot, 2013; 45: 6–14.

[20] Abramovich GN. The theory of turbulent jets. Cambridge, MA: MIT Press, 1963; 671p.
[21] Li C, Zhang X, Jiang J, Hu Y. Development and experiment of riser air-blowing sprayer in vineyard. Transactions of the CSAE, 2013; 29(4): 71–78. (in Chinese)
[22] Falcao L D, Chaves E S, Burin V M, Falcao A P, Gris E F, Bonin V, et al. Maturity of Cabernet Sauvignon berries from grapevines grown with two different training systems in a new grape growing region in Brazil. Ciencia E Investigacion Agraria, 2008; 35(3): 321–332.
[23] Fox R D, Brazee R D, Svensson S A, Reichard D L. Air jet velocities from a cross-flow fan sprayer. Transactions of the ASAE, 1992; 35(5): 1381–1382.
[24] Moslehi F, Ligas J R, Pisani M A, Epstein M A F. The unsteady form of the Bernoulli equation for estimating pressure-drop in the airways. Respiration Physiology, 1989; 76(3): 319–326.
[25] Qin R Q, Duan C Y. The principle and applications of Bernoulli equation. Journal of Physics: Conference Series, 2017; 916: 012038. doi: 10.1088/1742-6596/916/1/012038.
[26] Cohen J, Marasli B, Levinski V. The interaction between the mean flow and coherent structures in turbulent mixing layers. J Fluid Mech, 1994; 260: 81–94.
[27] Walker D T, Chen C Y, Willmarth WW. Turbulent structure in free-surface jet flows. J Fluid Mech, 1995; 291: 223–261.
[28] Hollingsworth D K, Bourgogne H A. The development of a turbulent boundary layer in high free-stream turbulence produced by a tow-stream mixing layer. Exp Thermal and Fluid Sci, 1995; 11(2): 210–222.
[29] Dai F. Selection and calculation of the blowing rate of air-assisted sprayers. Plant Prot, 2008; 6: 124–127. (in Chinese)
[30] Lazzarotto L, Lazzaretto A, Martegani A D, Macor A. On cross-flow fan similarity: Effects of casing shape. J Fluids Eng-Trans ASME, 2001; 123(3): 523–531.
[31] Lazzaretto A. A criterion to define cross-flow fan design parameters. J Fluids Eng-Trans ASME, 2003; 125(4): 680–683.
[32] Lazzaretto A, Toffolo A, Martegani A D. A systematic experimental approach to cross-flow fan design. J Fluids Eng-Trans ASME, 2003; 125(4): 684–693.
[33] Toffolo A, Lazzaretto A, Martegani A D. Cross-flow fan design guidelines for multi-objective performance optimization. Proc Inst Mech Eng Part a-J Power and Energy, 2004; 218(A1): 33–42.
[34] Toffolo A. On the theoretical link between design parameters and performance in cross-flow fans: a numerical and experimental study. Comput & Fluids, 2005; 34(1): 49–66.
[35] He X K. Pesticide equipment and application technology. Beijing: China Agricultural University Press, 2013. (in Chinese)